Trimerization of Alkali Dicyanamides $M[N(CN)_2]$ and Formation of Tricyanomelaminates $M_3[C_6N_9]$ (M = K, Rb) in the Melt: Crystal Structure Determination of Three Polymorphs of $K[N(CN)_2]$, Two of $Rb[N(CN)_2]$, and One of $K_3[C_6N_9]$ and $Rb_3[C_6N_9]$ from X-ray Powder Diffractometry

Elisabeth Irran, Barbara Jürgens, and Wolfgang Schnick*[a]

Abstract: The alkali dicyanamides $M[N(CN)_2]$ (M = K, Rb) were synthesized through ion exchange, and the corresponding tricyanomelaminates $M_3[C_6N_9]$ were obtained by heating the respective dicyanamides. The thermal behavior of the dicyanamides and their reaction to form the tricyanomelaminates were investigated by temperature-dependent X-ray powder diffractometry and thermoanalytical measurements. Potassium dicyanamide $K[N(CN)_2]$ was found to undergo four phase transitions: At 136 °C the low-temperature modification α-$K[N(CN)_2]$ transforms to β-$K[N(CN)_2]$, and at 187 °C the latter transforms to the high-temperature modification γ-$K[N(CN)_2]$, which melts at 232 °C. Above 310 °C the dicyanamide ions $[N(CN)_2]^-$ trimerize and the resulting tricyanomelaminate $K_3[C_6N_9]$ solidifies. Two modifications of rubidium dicyanamide have been identified: Even at −25 °C, the α form slowly transforms to β-$Rb[N(CN)_2]$ within weeks. $Rb[N(CN)_2]$ has a melting point of 190 °C. Above 260 °C the dicyanamide ions $[N(CN)_2]^-$ of the rubidium salt trimerize in the melt and the tricyanomelaminate $Rb_3[C_6N_9]$ solidifies. The crystal structures of all phases were determined by powder diffraction methods and were refined by the Rietveld method. α-$K[N(CN)_2]$ (*Pbcm*, $a = 836.52(1)$, $b = 646.90(1)$, $c = 721.27(1)$ pm, $Z = 4$), γ-$K[N(CN)_2]$ (*Pnma*, $a = 855.40(3)$, $b = 387.80(1)$, $c = 1252.73(4)$ pm, $Z = 4$), and β-$Rb[N(CN)_2]$ (*C2/c*, $a = 1381.56(2)$, $b = 1000.02(1)$, $c = 1443.28(2)$ pm, $\beta = 116.8963(6)°$, $Z = 16$) represent new structure types. The crystal structure of β-$K[N(CN)_2]$ ($P2_1/n$, $a = 726.92(1)$, $b = 1596.34(2)$, $c = 387.037(5)$ pm, $\beta = 111.8782(6)°$, $Z = 4$) is similar but not isotypic to the structure of α-$Na[N(CN)_2]$. α-$Rb[N(CN)_2]$ (*Pbcm*, $a = 856.09(1)$, $b = 661.711(7)$, $c = 765.067(9)$ pm, $Z = 4$) is isotypic with α-$K[N(CN)_2]$. The alkali dicyanamides contain the bent planar anion $[N(CN)_2]^-$ of approximate symmetry C_{2v} (average bond lengths: $C-N_{bridge}$ 133, $C-N_{term}$ 113 pm; average angles N-C-N 170°, C-N-C 120°). $K_3[C_6N_9]$ ($P2_1/c$, $a = 373.82(1)$, $b = 1192.48(5)$, $c = 2500.4(1)$ pm, $\beta = 101.406(3)°$, $Z = 4$) and $Rb_3[C_6N_9]$ ($P2_1/c$, $a = 389.93(2)$, $b = 1226.06(6)$, $c = 2547.5(1)$ pm, $\beta = 98.741(5)°$, $Z = 4$) are isotypic and they contain the planar cyclic anion $[C_6N_9]^{3-}$. Although structurally related, $Na_3[C_6N_9]$ is not isotypic with the tricyanomelaminates $M_3[C_6N_9]$ (M = K, Rb).

Keywords: dicyanamides · nitrides · phase transitions · structure elucidation · tricyanomelaminates

Introduction

The interest in carbon nitride chemistry has increased continuously during the last few years, although the existence of carbon nitride C_3N_4 as well as the material properties of this binary nitride are still under controversial discussion.[1] Simple alkali or alkaline earth salts like the cyanamides (e.g., $M^{II}[CN_2]$)[2] or the dicyanamides (e.g., $M^I[N(CN)_2]$ or $M^{II}[N(CN)_2]_2$)[3, 4] may be understood as simple and less condensed ternary nitridocarbonates(IV) derived from the binary parent compound C_3N_4. These compounds have been discussed already as be suitable as starting materials for the synthesis of C_3N_4. For example, the reaction of alkali dicyanamides with cyanuric chloride ($C_3N_3Cl_3$) may lead to the formation of carbon nitride[5] [cf. Eq. (1)].

$$3\,M^I[N(CN)_2] + C_3N_3Cl_3 \longrightarrow 3\,M^ICl + 3\,C_3N_4 \quad (1)$$

Although sodium dicyanamide $Na[N(CN)_2]$ is commercially available, detailed information about its crystal structure and thermal properties have not been available until recently.[3] Early investigations[6] gave evidence for a thermally induced trimerization of $Na[N(CN)_2]$ to form sodium tricyanomelaminate, $Na_3[C_6N_9]$ [cf. Eq. (2)]. The latter contains the s-triazine ring system (C_3N_3). Similar behaviour has been observed for $Li[N(CN)_2]$.[5]

[a] Prof. Dr. W. Schnick, Mag. E. Irran, Dipl.-Chem. B. Jürgens
Department Chemie, Ludwig-Maximilians-Universität
Butenandtstrasse 5–13 (Haus D), 81377 München (Germany)
Fax: (+49) 89-2180-7440
E-mail: wsc@cup.uni-muenchen.de

  0947-6539/01/0724-5372 $ 17.50+.50/0

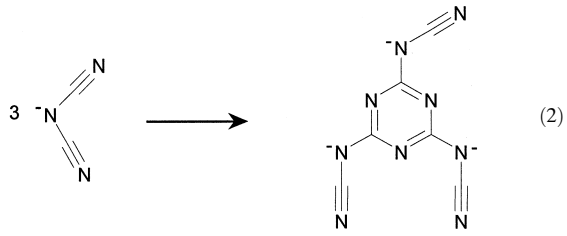

(2)

The s-triazine ring system (C_3N_3) is a structural feature of many heterocycles, for example, 2,4,6-triamino-s-triazine (melamine), $C_3N_3(NH_2)_3$, and 2,4,6-trichloro-s-triazine (cyanuric chloride), $C_3N_3Cl_3$. Furthermore, there is evidence that C_3N_3 rings are a basic structural feature of the so-called compounds melam, $H_9C_6N_{11}$, and melon, $(HC_2N_3)_x$, as well as the graphitic form of carbon nitride, g-C_3N_4.[7–9] For these compounds synthetic procedures have been reported; however, their true nature is still unknown.[10–12] Therefore detailed knowledge about the C_3N_3 ring formation is of special interest.

Recently, the existence of two polymorphs of sodium dicyanamide, α- and β-$Na[N(CN)_2]$, and details of the formation of $Na_3[C_6N_9]$ have been reported.[3] Thermoanalytical investigations (differential thermal analysis and differential scanning calorimetry) and temperature dependant X-ray diffraction studies gave evidence that the trimerization of $Na[N(CN)_2]$ to form $Na_3[C_6N_9]$ occurs in the solid phase and that there is no preorientation of the dicyanamide ions in the crystal before their transformation to tricyanomelaminate ions.[3]

Very recently, potassium tricyanomelaminate, $K_3[C_6N_9]$, was synthesized by the reaction of melamine with KSCN, and $K_3[C_6N_9]$ has been used for the synthesis of graphite-like carbon nitrides.[13] However, details concerning the formation and crystal structure of $K_3[C_6N_9]$ are not available as yet.

Herein we report on the synthesis and the crystal structures of polymorphic $K[N(CN)_2]$ and $Rb[N(CN)_2]$, and the trimerization of their anions $[N(CN)_2]^-$ to form $[C_6N_9]^{3-}$. To our knowledge these are the first examples in which simple inorganic anions trimerize in the melt.

Abstract in German: *Die Alkalidicyanamide M[N(CN)$_2$] (M = K, Rb) wurden durch Ionenaustausch synthetisiert, die Tricyanomelaminate $M_3[C_6N_9]$ durch Erhitzen des jeweiligen Dicyanamids. Das Temperaturverhalten der Dicyanamide und ihre Reaktion zu den Tricyanomelaminaten wurden durch temperaturabhängige Röntgen-Pulverdiffraktometrie und thermoanalytische Messungen untersucht. Für Kaliumdicyanamid K[N(CN)$_2$] wurden vier Phasenübergänge beobachtet: Bei 136 °C geht die Tieftemperaturmodifikation α-K[N(CN)$_2$] in β-K[N(CN)$_2$] über, bei 187 °C wandelt sich β-K[N(CN)$_2$] in die Hochtemperaturmodifikation γ-K[N(CN)$_2$] um, welches bei 232 °C schmilzt. Oberhalb 310 °C trimerisieren die Dicyanamid-Ionen $[N(CN)_2]^-$, und die Schmelze erstarrt unter Bildung von $K_3[C_6N_9]$. Von Rubidiumdicyanamid gibt es zwei Modifikationen: Die α-Form wandelt sich selbst bei −25 °C innerhalb von Wochen zu β-Rb[N(CN)$_2$] um. Rb[N(CN)$_2$] schmilzt bei 190 °C und wird oberhalb von 260 °C zu $Rb_3[C_6N_9]$, wobei die Schmelze erstarrt. Die Kristallstrukturen aller Phasen wurden mit Pulverbeugungsmethoden bestimmt und mit der Rietveld-Methode verfeinert. Die Kristallstruktur von α-K[N(CN)$_2$] (Pbcm, a = 836,52(1), b = 646,90(1), c = 721,27(1) pm, Z = 4) und γ-K[N(CN)$_2$] (Pnma, a = 855,40(3), b = 387,80(1), c = 1252,73(4) pm, Z = 4) sowie von β-Rb[N(CN)$_2$] (C2/c, a = 1381,56(2), b = 1000,02(1), c = 1443,28(2) pm, β = 116,8963(6)°, Z = 16) stellen neue Strukturtypen dar. Die Kristallstruktur von β-K[N(CN)$_2$] ($P2_1/n$, a = 726,92(1), b = 1596,34(2), c = 387,037(5) pm, β = 111,8782(6)°, Z = 4) ähnelt der Struktur von α-Na[N(CN)$_2$], beide sind aber nicht isotyp. α-Rb[N(CN)$_2$] (Pbcm, a = 856,09(1), b = 661,711(7), c = 765,067(9) pm, Z = 4) ist isotyp zu α-K[N(CN)$_2$]. Die Alkalidicyanamide enthalten das gewinkelte Anion $[N(CN)_2]^-$ mit annähernder Punktsymmetrie C_{2v} (durchschnittliche Abstände C–$N_{verbrückend}$ 133 pm, C–$N_{terminal}$ 113 pm; durchschnittliche Winkel N-C-N 170°, C-N-C 120°). $K_3[C_6N_9]$ ($P2_1/c$, a = 373,82(1), b = 1192,48(5), c = 2500,4(1) pm, β = 101,406(3)°, Z = 4) und $Rb_3[C_6N_9]$ ($P2_1/c$, a = 389,93(2), b = 1226,06(6), c = 2547,5(1) pm, β = 98,741(5)°, Z = 4) sind isotyp und enthalten planare cyclische Anionen $[C_6N_9]^{3-}$. Ihre Kristallstrukturen sind mit der von $Na_3[C_6N_9]$ verwandt, aber nicht isotyp dazu.*

Experimental Section

General techniques: The tricyanomelaminates $M_3[C_6N_9]$ (M = K, Rb) are hygroscopic and form the monohydrates $M_3[C_6N_9]\cdot H_2O$. Thus the syntheses of $M_3[C_6N_9]$ were carried out under an atmosphere of dried argon.

Potassium and rubidium dicyanamide were prepared by ion exchange: A column filled with a resin (Merck, Ionenaustauscher I, Art. 4765) was filled with an aqueous solution of KCl (Merck, p. A.) or RbCl (Alfa Aesar, 99 %), respectively. The column was washed with water until the eluate was free of Cl^- ions. An aqueous solution of sodium dicyanamide $Na[N(CN)_2]$ (Fluka, ≥ 96 %) was poured onto the column. The eluate was collected and, after drying at 8 °C, the low-temperature phase α-$K[N(CN)_2]$ was isolated, whereas evaporation of the water at 20 °C led to the formation of β-$K[N(CN)_2]$. The high-temperature modification γ-$K[N(CN)_2]$ was obtained during heating of $K[N(CN)_2]$ to 200 °C. The high-temperature polymorph γ-$K[N(CN)_2]$ was quenched to room temperature without retransformation. By drying a solution of rubidium dicyanamide at 20 °C both α- and β-$Rb[N(CN)_2]$ were obtained. After a period of several days at ambient conditions the X-ray diffraction peaks of α-$Rb[N(CN)_2]$ disappeared, indicating that single-phase β-$Rb[N(CN)_2]$ had formed. $Rb[N(CN)_2]$ exhibited a melting point of 190 °C. Rapid quenching (100 °C min^{-1}) of the melt to 0 °C led to the formation of single-phase α-$Rb[N(CN)_2]$.

The tricyanomelaminates $K_3[C_6N_9]$ and $Rb_3[C_6N_9]$ were obtained by heating the respective dicyanamides $M[N(CN)_2]$ (M = K, Rb) in sealed duran ampoules under argon up to 380 °C ($K_3[C_6N_9]$) and 400 °C ($Rb_3[C_6N_9]$), respectively. The thermally induced process was checked visually: The colorless dicyanamide powders first transform to light brown melts and solidify with further heating. After cooling to room temperature, the $M_3[C_6N_9]$ salts were obtained as microcrystalline, light gray powders. Samples of $Rb_3[C_6N_9]$ were synthesized with better crystallinity by ion exchange, starting from $Na_3[C_6N_9]$. A solution of $Na_3[C_6N_9]$ was poured onto a column filled with an ion-exchange resin that had been loaded with Rb^+ ions. The eluate was collected and dried at room temperature leading to the triclinic monohydrate $Rb_3[C_6N_9]\cdot H_2O$, which has been structurally characterized by X-ray synchrotron powder diffraction.[14] Anhydrous $Rb_3[C_6N_9]$ was obtained as a white microcrystalline powder by heating $Rb_3[C_6N_9]\cdot H_2O$ to 350 °C (heating rate: 5 °C min^{-1}) under vacuum (10^{-2} mbar). $K_3[C_6N_9]$ was also synthesized by dehydrating the monohy-

drate, which is isotypic with $Rb_3[C_6N_9]\cdot H_2O$. However, the crystallinity of the samples obtained by thermal trimerization was better than that of the product obtained by using this procedure.

Thermal analysis: Differential scanning calorimetry (DSC) curves of $K[N(CN)_2]$ and $Rb[N(CN)_2]$ were recorded with a Mettler DSC 25. α-$K[N(CN)_2]$ was heated from 0 to 500 °C (heating rate: 10 °C min^{-1}, sample weight: 34.9 mg) (Figure 1). The insert of Figure 1 shows the enlarged thermal effects between 90 and 220 °C. A DSC curve of β-$Rb[N(CN)_2]$ was recorded up to 500 °C (heating rate: 10 °C min^{-1}, sample weight: 41.5 mg) (Figure 2).

X-ray diffraction: X-ray powder diffraction data were used for the crystal structure determination. The diffraction investigations were carried out on a conventional powder diffractometer (STOE Stadi P, $Cu_{K\alpha 1}$ radiation) in Debye–Scherrer geometry. The diffraction patterns were indexed by the program ITO;[15] the space groups determined by using systematic extinction rules and confirmed by the successful structure refinement (Tables 1 and 2).

The crystal structures of α-$K[N(CN)_2]$, γ-$K[N(CN)_2]$, and β-$Rb[N(CN)_2]$ were solved by direct methods by using the programs EXTRA[16] and SIRPOW.[17] The diffraction pattern and the lattice constants of β-$K[N(CN)_2]$ were similar to those of α-$Na[N(CN)_2]$,[3] while the lattice constants of α-$Rb[N(CN)_2]$ resemble those of α-$K[N(CN)_2]$. Therefore the atomic coordinates of α-$Na[N(CN)_2]$ and of α-$K[N(CN)_2]$ were used as starting parameters for the Rietveld refinement of β-$K[N(CN)_2]$ and α-$Rb[N(CN)_2]$, respectively, which were performed with the program GSAS.[18]

Both $Na_3[C_6N_9]$ and $K_3[C_6N_9]$ crystallize in the monoclinic space group $P2_1/c$ and their lattice constants are similar: ($Na_3[C_6N_9]$ ($P2_1/c$): $a = 351.616(3)$, $b = 2338.06(3)$, $c = 1112.34(1)$ pm, $\beta = 100.333(9)°$;[3] $K_3[C_6N_9]$ ($P2_1/c$): $a = 373.82(2)$, $b = 1192.48(5)$, $c = 2500.4(1)$ pm, $\beta = 101.406(3)°$). In contrast to $Na_3[C_6N_9]$, the β angle in $K_3[C_6N_9]$ encloses the shortest and the longest lattice constant. Therefore the unit cells of the two compounds are similar but not strictly isomorphous. However, the similarity of the diffraction patterns of both compounds indicates a close relationship between their crystal structures. An ab-initio structure determination of $K_3[C_6N_9]$ by using direct methods revealed that the K^+ ions exhibited atomic coordination similar to that observed for the Na^+ ions in $Na_3[C_6N_9]$, but with the y and z

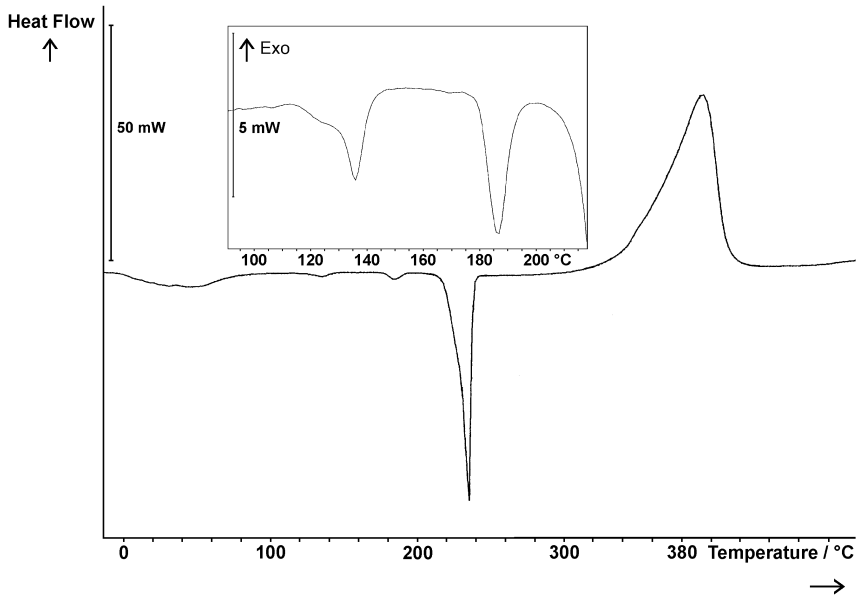

Figure 1. DSC curve of $K[N(CN)_2]$: melting of $K[N(CN)_2]$ and trimerization to $K_3[C_6N_9]$. Insert: phase transitions of α-$K[N(CN)_2]$ to β-$K[N(CN)_2]$ and to γ-$K[N(CN)_2]$.

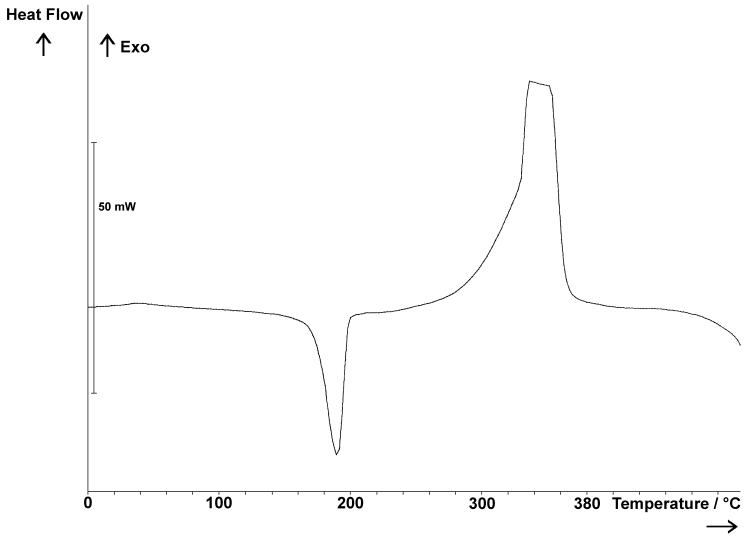

Figure 2. DSC curve of β-$Rb[N(CN)_2]$: melting and trimerization to $Rb_3[C_6N_9]$.

Table 1. Crystallographic data for α-$K[N(CN)_2]$, β-$K[N(CN)_2]$, γ-$K[N(CN)_2]$, and $K_3[C_6N_9]$.

	α-$K[N(CN)_2]$	β-$K[N(CN)_2]$	γ-$K[N(CN)_2]$	$K_3[C_6N_9]$
M_r [g mol^{-1}]	105.09	105.09	105.09	315.27
space group	*Pbcm* (no. 57)	$P2_1/n$ (no. 14)	*Pnma* (no. 62)	$P2_1/c$ (no. 14)
radiation, λ [pm]		$Cu_{K\alpha 1}$, 154.06		
a [pm]	836.52(1)	726.92(1)	855.40(3)	373.82(1)
b [pm]	646.90(1)	1596.34(2)	387.80(1)	1192.48(5)
c [pm]	721.27(1)	387.037(5)	1252.73(4)	2500.4(1)
β [°]		111.8782(6)		101.406(3)
V [10^6 pm]	390.31(1)	416.78(1)	415.57(3)	1092.63(9)
Z	4	4	4	4
ρ_{calcd} [g cm^{-3}]	1.789	1.676	1.680	1.918
profile range [°]	$5 \le 2\theta \le 90$	$5 \le 2\theta \le 90$	$5 \le 2\theta \le 80$	$3 \le 2\theta \le 80$
data points	8500	8500	7500	7700
observed reflections	176	342	155	658
atomic parameters	11	18	12	54
displacement factors	6	6	3	5
profile parameters	16	17	17	16
wR_p	0.053	0.065	0.082	0.067
R_p	0.041	0.051	0.061	0.053
R_F	0.064	0.082	0.081	0.034

0947-6539/01/0724-5374 $ 17.50+.50/0 *Chem. Eur. J.* **2001**, *7*, No. 24

Table 2. Crystallographic data for α-Rb[N(CN)$_2$], β-Rb[N(CN)$_2$], and Rb$_3$[C$_6$N$_9$].

	α-Rb[N(CN)$_2$]	β-Rb[N(CN)$_2$]	Rb$_3$[C$_6$N$_9$]
M_r [g mol^{-1}]	151.51	151.51	454.53
space group	*Pbcm* (no. 57)	*C*2/*c* (no. 15)	*P*2$_1$/*c* (no. 14)
radiation, λ [pm]		Cu$_{K\alpha1}$, 154.06	
a [pm]	856.09(1)	1381.56(2)	389.93(2)
b [pm]	661.711(7)	1000.02(1)	1226.06(6)
c [pm]	765.067(9)	1443.28(2)	2547.5(1)
β [°]		116.8963(6)	98.741(5)
V [10^6 pm]	433.399(8)	1778.31(4)	1203.7(1)
Z	4	16	4
ρ_{calcd} [g cm^{-3}]	2.320	2.263	2.508
profile range [°]	$5 \le 2\theta \le 90$	$5 \le 2\theta \le 90$	$5 \le 2\theta \le 80$
data points	8500	8500	7500
observed reflections	191	722	737
atomic parameters	11	36	54
displacement factors	6	12	5
profile parameters	18	16	17
wR_p	0.084	0.084	0.071
R_p	0.067	0.066	0.057
R_F	0.080	0.064	0.034

coordinates interchanged. Consequently a Rietveld refinement of K$_3$[C$_6$N$_9$] was carried out utilizing the positional parameters of Na$_3$[C$_6$N$_9$] as starting parameters with interchanged *y* and *z* coordinates. As the diffraction peaks of K$_3$[C$_6$N$_9$] were rather broad, it was necessary to use soft constraints for the bond lengths within the anion when refining the C and N positions (C–N$_{term}$ 113(1) and C–N$_{bridge}$ 135(1) pm) and the angles N-C-N (172(2)° within the arms of the anion, 120(2)° for all other angles) and C-N-C (120(2)°).

The diffraction pattern of Rb$_3$[C$_6$N$_9$] was indexed with slightly larger lattice constants relative to those of K$_3$[C$_6$N$_9$], and thus an isotypic structure was assumed. Starting from the atomic coordinates of K$_3$[C$_6$N$_9$] the Rietveld refinement of Rb$_3$[C$_6$N$_9$] was straightforward, but the application of soft constraints for the bond lengths was also necessary. The monoclinic unit cell of Rb$_3$[C$_6$N$_9$] can be transformed into a pseudo-orthorhombic cell (a = 389.93(2), b = 1226.02(6), c = 2517.84(2) pm, β = 90.067(6)°), but the orthorhombic symmetry definitely was excluded by the structure refinement.

The atomic coordinates of the compounds are listed in Tables 3–7, and the refined powder diffraction patterns are shown in Figures 3–5.[19]

To investigate the phase transitions of K[N(CN)$_2$] and Rb[N(CN)$_2$], temperature dependent X-ray powder diffraction experiments were performed with a computer-controlled furnace on a STOE Stadi P diffractometer (Mo$_{K\alpha1}$ radiation) in Debye–Scherrer geometry (Figure 6). The temperature steps were 20 °C and the heating ramp was 50 °C min^{-1}. Furthermore, low-temperature X-ray diffraction investigations were performed with a 600 Series Cryostream Cooler, Oxford Cryosystems. However, no phase transitions between room temperature and 105 K were identified for K[N(CN)$_2$] and Rb[N(CN)$_2$].

Table 3. Atomic coordinates and displacement factors [pm^2] for α-K[N(CN)$_2$] and α-Rb[N(CN)$_2$] (first and second line, respectively).

Atom	Wyckoff position	*x*	*y*	*z*	U_{iso}[a]
K	4*c*	0.6825(2)	¼	0	479(5)
Rb	4*c*	0.6863(2)	¼	0	565(4)
C1	4*d*	0.066(1)	0.137(1)	¼	624(33)
	4*d*	0.073(2)	0.155(2)	¼	310(50)
C2	4*d*	0.319(1)	0.269(2)	¼	489(24)
	4*d*	0.319(2)	0.268(3)	¼	520(40)
N1	4*d*	−0.0694(8)	0.1467(8)	¼	581(28)
	4*d*	−0.055(1)	0.146(1)	¼	650(50)
N2	4*d*	0.2187(8)	0.1079(9)	¼	503(25)
	4*d*	0.218(1)	0.116(2)	¼	400(40)
N3	4*d*	0.4193(9)	0.3871(9)	¼	415(25)
	4*d*	0.418(1)	0.384(2)	¼	370(40)

[a] U_{iso} is defined as $\exp(-8\pi^2 U_{iso}\sin^2\theta/\lambda^2)$.

Table 4. Atomic coordinates and displacement factors [pm^2] for β-K[N(CN)$_2$].

Atom	Wyckoff position	*x*	*y*	*z*	U_{iso}[a]
K	4*e*	0.6766(3)	0.09599(9)	0.3330(5)	587(6)
C1	4*e*	0.164(1)	0.0879(5)	0.127(2)	731(30)
C2	4*e*	0.0410(9)	0.2125(4)	0.180(2)	537(27)
N1	4*e*	0.267(1)	0.0392(4)	0.112(2)	807(26)
N2	4*e*	0.0097(7)	0.1370(3)	0.063(1)	596(24)
N3	4*e*	0.0564(7)	0.2843(3)	0.244(1)	490(23)

[a] U_{iso} is defined as $\exp(-8\pi^2 U_{iso}\sin^2\theta/\lambda^2)$.

Table 5. Atomic coordinates and displacement factors [pm^2] for γ-K[N(CN)$_2$].

Atom	Wyckoff position	*x*	*y*	*z*	U_{iso}[a]
K	4*c*	0.1245(4)	¼	0.6292(4)	657(18)
C1	4*c*	0.514(2)	¼	0.372(2)	750(50)
C2	4*c*	0.234(2)	¼	0.387(2)	750(50)
N1	4*c*	0.637(5)	¼	0.396(1)	534(27)
N2	4*c*	0.372(2)	¼	0.324(1)	534(27)
N3	4*c*	0.117(5)	¼	0.399(1)	534(27)

[a] U_{iso} is defined as $\exp(-8\pi^2 U_{iso}\sin^2\theta/\lambda^2)$; the displacement factors of C and N were constrained to be equal.

Table 6. Atomic coordinates and displacement factors [pm^2] for β-Rb[N(CN)$_2$].

Atom	Wyckoff position	*x*	*y*	*z*	U_{iso}[a]
Rb1	8*f*	0.1654(1)	0.0078(2)	0.3709(1)	608(6)
Rb2	8*f*	0.5190(2)	0.1816(2)	0.0856(1)	707(7)
C1	8*f*	0.112(1)	0.046(2)	0.109(1)	430(60)
C2	8*f*	0.261(2)	0.153(2)	0.125(1)	710(70)
C3	8*f*	0.141(2)	0.333(2)	0.381(2)	1080(90)
C4	8*f*	0.151(2)	0.366(2)	0.226(2)	1010(90)
N1	8*f*	0.0604(9)	−0.014(1)	0.1415(9)	580(50)
N2	8*f*	0.165(1)	0.108(1)	0.0633(8)	260(50)
N3	8*f*	0.349(1)	0.201(1)	0.1664(9)	500(50)
N4	8*f*	0.139(1)	0.369(1)	0.455(1)	1020(70)
N5	8*f*	0.165(2)	0.302(2)	0.307(2)	2090(110)
N6	8*f*	0.139(1)	0.424(1)	0.152(1)	650(60)

[a] U_{iso} is defined as $\exp(-8\pi^2 U_{iso}\sin^2\theta/\lambda^2)$.

Results

Thermal behavior of K[N(CN)$_2$]: Below 200 °C the DSC curve of K[N(CN)$_2$] shows two small endothermic peaks (Figure 1). With reference to the in-situ X-ray powder diffractometry (Figure 6), the first peak at 136 °C (onset: 115 °C) belongs to the phase transition of α- to β-K[N(CN)$_2$] and the second at 187 °C (onset: 170 °C) indicates the phase transition of β- to γ-K[N(CN)$_2$]. Both phase transitions occur in the solid state.

Above 230 °C the DSC curve exhibits a large endothermic peak that indicates the melting of K[N(CN)$_2$] (Figure 1). According to X-ray powder diffractometry, the compound becomes X-ray amorphous above this temperature. γ-K[N(CN)$_2$] is obtained by slow cooling (1 °C min^{-1}) of the melt. When the melt is heated above 310 °C a broad exothermic peak (max. 400 °C) occurs, which belongs to the trimerization of the anions and the formation of K$_3$[C$_6$N$_9$]. Above 500 °C decomposition of K$_3$[C$_6$N$_9$] occurs.

Table 7. Atomic coordinates and displacement factors [pm^2] for $K_3[C_6N_9]$ and $Rb_3[C_6N_9]$ (first and second line, respectively).

Atom	Wyckoff position	x	y	z	U_{iso}[a]
K1	4*e*	0.560(1)	0.4149(4)	0.1013(2)	567(22)
Rb1	4*e*	0.553(2)	0.4109(3)	0.1019(2)	577(16)
K2	4*e*	0.546(1)	0.3512(4)	0.4863(2)	534(20)
Rb2	4*e*	0.518(2)	0.3481(3)	0.4850(1)	585(19)
K3	4*e*	0.397(1)	0.4961(4)	0.2584(2)	363(17)
Rb3	4*e*	0.427(1)	0.4870(4)	0.2579(2)	596(18)
C1	4*e*	0.037(3)	0.3607(8)	0.3523(5)	487(31)
	4*e*	0.038(4)	0.3500(9)	0.3511(6)	80(40)
C2	4*e*	0.003(3)	0.1740(9)	0.3823(5)	487(31)
	4*e*	0.031(4)	0.1700(9)	0.3811(6)	80(40)
C3	4*e*	0.078(3)	0.2116(7)	0.2951(5)	487(31)
	4*e*	0.052(5)	0.2052(9)	0.2919(6)	80(40)
C4	4*e*	−0.093(3)	0.513(1)	0.4025(5)	487(31)
	4*e*	−0.041(8)	0.502(1)	0.4051(6)	80(40)
C5	4*e*	−0.043(5)	0.131(1)	0.4720(5)	487(31)
	4*e*	0.016(4)	0.125(1)	0.4696(5)	80(40)
C6	4*e*	0.141(3)	0.254(1)	0.2076(4)	487(31)
	4*e*	0.122(3)	0.241(1)	0.2047(5)	80(40)
N1	4*e*	−0.012(3)	0.2867(9)	0.3923(5)	205(18)
	4*e*	−0.019(5)	0.2774(9)	0.3888(6)	247(28)
N2	4*e*	0.026(3)	0.1367(8)	0.3322(4)	205(18)
	4*e*	0.025(5)	0.134(1)	0.3311(6)	247(28)
N3	4*e*	0.002(3)	0.3184(8)	0.3017(5)	205(18)
	4*e*	0.036(5)	0.3131(9)	0.3012(6)	247(28)
N4	4*e*	−0.079(3)	0.4677(8)	0.3544(4)	205(18)
	4*e*	−0.031(5)	0.4570(9)	0.3570(6)	247(28)
N5	4*e*	−0.054(4)	0.0991(8)	0.4198(5)	205(18)
	4*e*	−0.043(5)	0.098(1)	0.4177(5)	247(28)
N6	4*e*	0.071(4)	0.1777(7)	0.2444(5)	205(18)
	4*e*	0.057(5)	0.169(1)	0.2421(6)	247(28)
N7	4*e*	−0.147(3)	0.546(1)	0.4424(4)	205(18)
	4*e*	−0.061(8)	0.551(1)	0.4419(6)	247(28)
N8	4*e*	−0.061(4)	0.147(1)	0.5161(5)	205(18)
	4*e*	0.032(8)	0.155(1)	0.5117(5)	247(28)
N9	4*e*	0.152(4)	0.315(1)	0.1738(5)	205(18)
	4*e*	0.137(7)	0.299(2)	0.1707(6)	247(28)

[a] U_{iso} is defined as $\exp(-8\pi^2 U_{iso}\sin^2\theta/\lambda^2)$; the displacement factors of C and N were constrained to be equal.

α-K[N(CN)$_2$]: According to the crystal structure determination α-K[N(CN)$_2$] is built up by layers of $[N(CN)_2]^-$ ions (001) alternating with layers of K^+ ions (Figure 7). The K^+ ions are surrounded by four N atoms in the layer above and four in the layer below, to form a rather regular quadratic antiprism with an average K^+–N distance of 299 pm (Table 8). Two of these N atoms are bridging (N_{bridge}), while all others are terminal (N_{term}). The $[N(CN)_2]^-$ ion is planar and bent, and the horizontal mirror plane of the molecular anion coincides with a crystallographic mirror plane. Analogously to other dicyanamides, the symmetry of the anion is C_{2v}, and the C–N_{term} bond lengths are shorter than those to the bridging atoms (N_{bridge}). The crystal structure of α-K[N(CN)$_2$] resembles that of KSCN: Both compounds crystallize in the same space group and with similar lattice constants, except the *a* lattice constant.[20] In KSCN the K^+ and SCN^- ions are also arranged in alternating layers. The S and N atoms form a quadratic antiprism around K^+ as the N atoms do in α-K[N(CN)$_2$]. Replacement of the N1-C1-N2 groups by a single atom in α-K[N(CN)$_2$] nearly transforms the structure to that of KSCN. A similar relationship was found between the structures of Ca[N(CN)$_2$]$_2$ and Pb[SCN]$_2$.[4, 21]

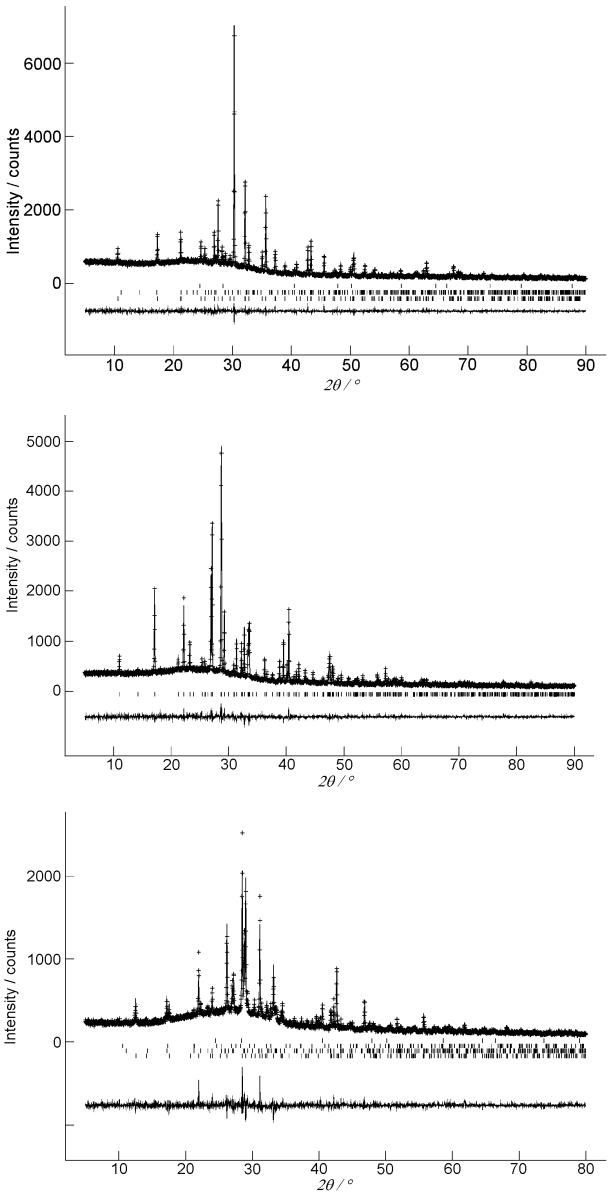

Figure 3. Top: Observed (crosses) and calculated (line) X-ray powder diffraction patterns as well as difference profile of the Rietveld refinement of α-K[N(CN)$_2$]. The lower row of vertical lines indicates possible peak positions, the upper rows indicate β-K[N(CN)$_2$] and KCl. Middle: Observed (crosses) and calculated (line) X-ray powder diffraction patterns as well as difference profile of the Rietveld refinement of β-K[N(CN)$_2$] (STOE Stadi P, $\lambda = 154.06$ pm). The row of vertical lines indicates possible peak positions. Bottom: Observed (crosses) and calculated (line) X-ray powder diffraction patterns as well as difference profile of the Rietveld refinement of γ-K[N(CN)$_2$] (STOE Stadi P, $\lambda = 154.06$ pm). The lower row of vertical lines indicates possible peak positions, the upper rows α-K[N(CN)$_2$], β-K[N(CN)$_2$], and KCl.

β-K[N(CN)$_2$]: The crystal structure of β-K[N(CN)$_2$] can be derived from the closely related structures of α- and β-Na[N(CN)$_2$].[3] In both polymorphs of Na[N(CN)$_2$] the Na^+ and $[N(CN)_2]^-$ ions are positioned in the same layer, and the horizontal mirror plane of the $[N(CN)_2]^-$ ion is nearly (α-Na[N(CN)$_2$]) or exactly (β-Na[N(CN)$_2$]) parallel (001), respectively. Both the cations and anions in β-K[N(CN)$_2$] are also arranged in layers, but the horizontal mirror planes of the $[N(CN)_2]^-$ ions now form a much larger angle with the (001)

0947-6539/01/0724-5376 $ 17.50+.50/0 *Chem. Eur. J.* **2001**, *7*, No. 24

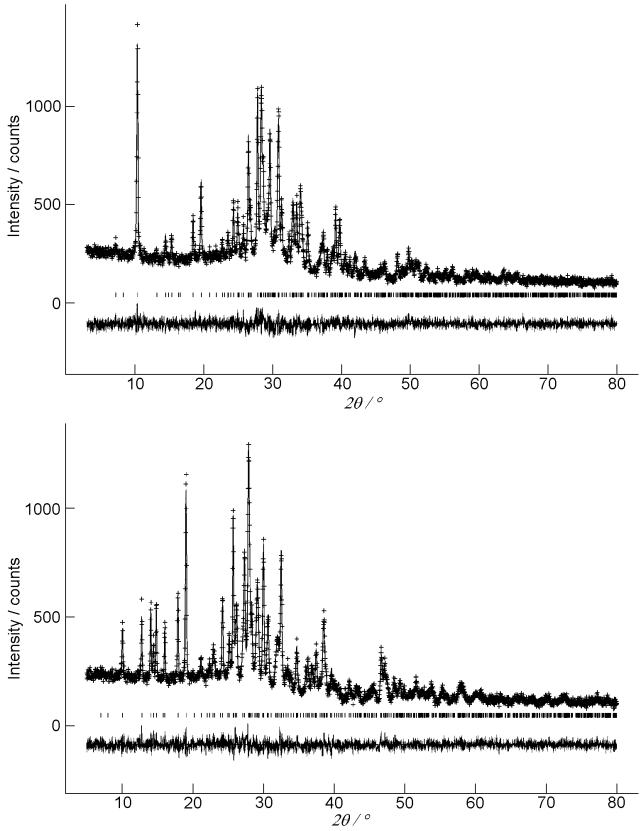

Figure 4. Top: Observed (crosses) and calculated (line) X-ray powder diffraction patterns as well as difference profile of the Rietveld refinement of $K_3[C_6N_9]$ (STOE Stadi P, $\lambda = 154.06$ pm). The row of vertical lines indicates possible peak positions. Bottom: Observed (crosses) and calculated (line) X-ray powder diffraction patterns as well as difference profile of the Rietveld refinement of $Rb_3[C_6N_9]$ (STOE Stadi P, $\lambda = 154.06$ pm). The row of vertical lines indicates possible peak positions.

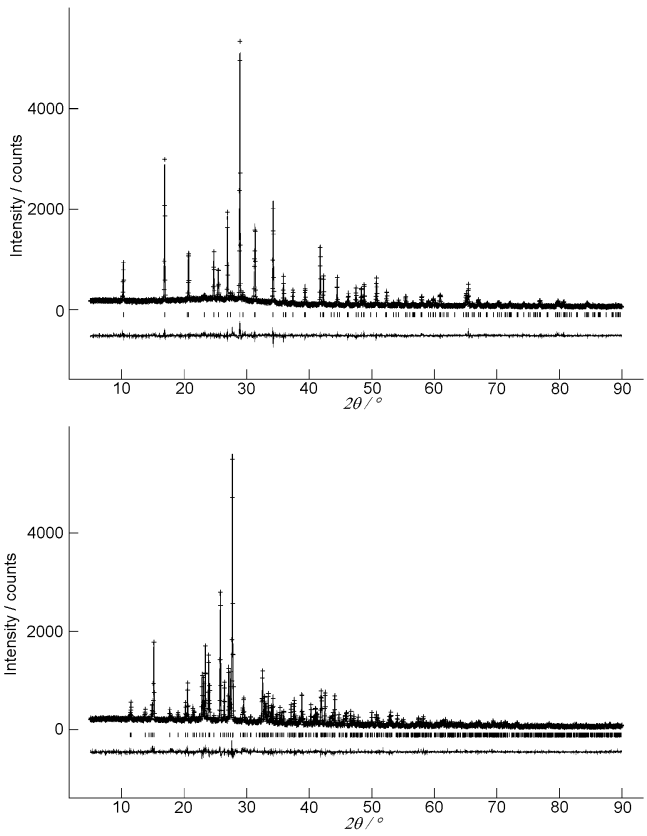

Figure 5. Top: Observed (crosses) and calculated (line) X-ray powder diffraction patterns as well as difference profile of the Rietveld refinement of α-$Rb[N(CN)_2]$ (STOE Stadi P, $\lambda = 154.06$ pm). The row of vertical lines indicates possible peak positions. Bottom: Observed (crosses) and calculated (line) X-ray powder diffraction patterns as well as difference profile of the Rietveld refinement of β-$Rb[N(CN)_2]$ (STOE Stadi P, $\lambda = 154.06$ pm). The row of vertical lines indicates possible peak positions.

plane (Figure 8). This tilt enables the K^+ to be coordinated by a further N_{bridge} atom. In contrast to $Na[N(CN)_2]$, in which the cations are coordinated by six N atoms, the K^+ ions in β-$K[N(CN)_2]$ thus are surrounded by seven N atoms with an average K^+–N distance of 292 pm (Table 9). Due to the higher coordination number of the cations, β-$K[N(CN)_2]$ cannot be called isotypic with α-$Na[N(CN)_2]$. This structural feature is also documented by the positional parameters: In contrast to α-$Na[N(CN)_2]$ the z coordinates in β-$K[N(CN)_2]$ deviate significantly from ¼.

γ-$K[N(CN)_2]$: The reversible phase transition between α- and β-$Na[N(CN)_2]$ at 33 °C was assumed to be almost second order because a close group–subgroup relation exists between both structures. Furthermore, only small shifts of the atomic coordinates are necessary to orientate the plane of the dicyanamides parallel (001) in β-$Na[N(CN)_2]$.[3] As the crystal structure of β-$K[N(CN)_2]$ and α-$Na[N(CN)_2]$ are very similar, a structure type similar to β-$Na[N(CN)_2]$ was expected for γ-$K[N(CN)_2]$. However, the crystal structure determination of γ-$K[N(CN)_2]$ proved that this is not the case.

Analogously to β-$Na[N(CN)_2]$ all atoms in γ-$K[N(CN)_2]$ are positioned on the mirror planes of the space group *Pnma*. Nevertheless the dicyanamide ions are arranged in a completely different way (Figure 9). In the [100] direction in

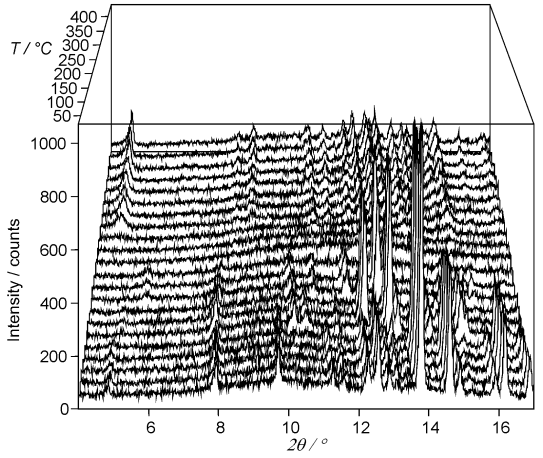

Figure 6. Temperature-dependent powder diffractometry of $K[N(CN)_2]$, $Mo_{K\alpha 1}$ radiation, 20–440 °C in steps of 20 °C.

γ-$K[N(CN)_2]$ all anions exhibit the same orientation, while in the respective [010] direction in β-$Na[N(CN)_2]$, successive dicyanamide ions are rotated about 180°. The K^+ ions are coordinated to seven N atoms, the average K^+–N distance is 293 pm (Table 9). Three of the N atoms are located in the layer above the K^+ layer, and three below. Together they form a trigonal prism around K^+, while a further N atom, which is

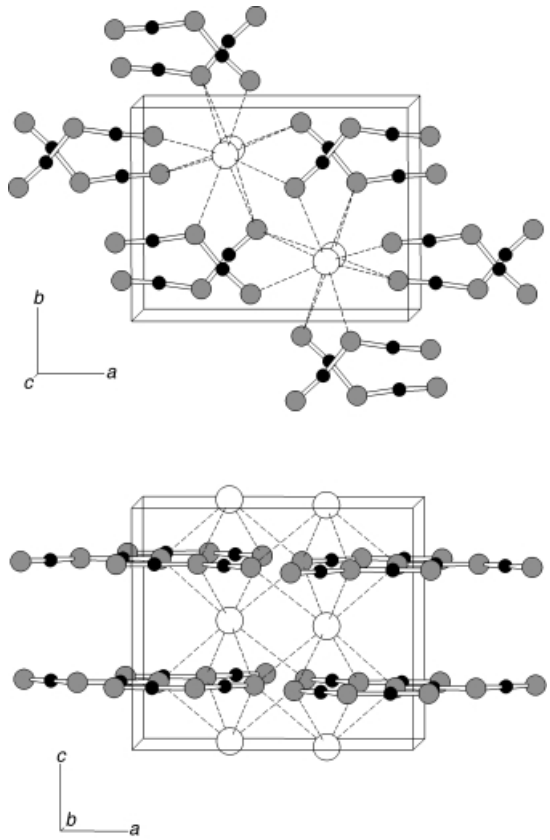

Figure 7. Top: Crystal structure of α-K[N(CN)$_2$], view along [001] (K: open circles, C: black circles, N: gray circles). The crystal structure of α-Rb[N(CN)$_2$] is analogous. Bottom: Crystal structure of α-K[N(CN)$_2$], view along [010] (K: open circles, C: black circles, N: gray circles).

Table 8. Interatomic distances [pm] and angles [°] in α-K[N(CN)$_2$] and α-Rb[N(CN)$_2$].

	α-K[N(CN)$_2$]	α-Rb[N(CN)$_2$]
M–N1	282.9(5) 2x	300.4(7) 2x
M–N2	304.9(5) 2x	319.4(9) 2x
M–N3	298.1(6) 2x	311.7(9) 2x
M–N3	308.0(5) 2x	321.5(9) 2x
C1–N1	114(1)	110(2)
C1–N2	129(1)	127(2)
C2–N2	134(1)	133(2)
C2–N3	114(1)	114(2)
C1-N2-C2	120.5(8)	119(1)
N1-C1-N2	175(1)	165(2)
N2-C2-N3	171(2)	173(2)

positioned in the same layer as the K^+ atom, caps a prism face. As for β-K[N(CN)$_2$], two of the N atoms which coordinate to the K^+ ions are bridging (N_{bridge}). The crystallographic point symmetry of the planar $[N(CN)_2]^-$ ion is C_s while the symmetry of the molecular anion is nearly C_{2v}.

In γ-K[N(CN)$_2$], the thermal expansion is normal for lattice constants b and c, whilst for lattice constant a it is negative. According to the Rietveld refinement of the diffraction pattern recorded at 190 °C, this is caused by the distortion of the polyhedron of the N atoms around the K^+ ion. Similar behavior was observed for the crystals of M[N(CN)$_2$]$_2$ (M = Mn, Co, Ni). Here the negative thermal expansion of one of the lattice constants is caused by a distortion and tilting of the octahedra of the N atoms around the cations.[22, 23]

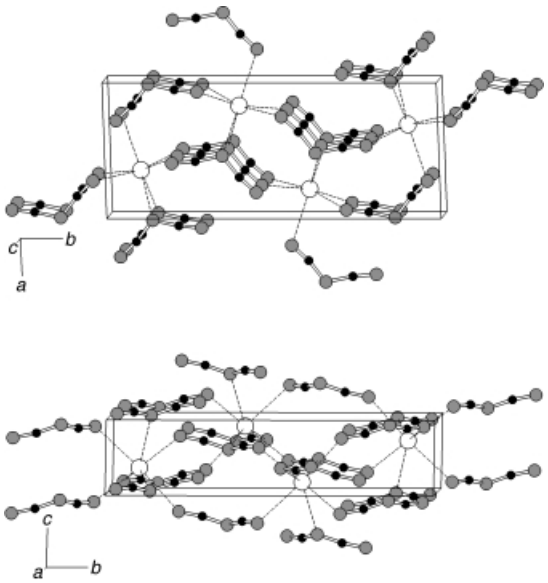

Figure 8. Top: Crystal structure of β-K[N(CN)$_2$], view along [001] (K: open circles, C: black circles, N: gray circles). Bottom: Crystal structure of β-K[N(CN)$_2$], view along [100] (K: open circles, C: black circles, N: gray circles).

Table 9. Interatomic distances [pm] and angles [°] in β-K[N(CN)$_2$], γ-K[N(CN)$_2$], and β-Rb[N(CN)$_2$].

β-K[N(CN)$_2$]			
K–N1	291.9(7)	K–N2	302.8(5)
K–N1	288.5(6)	K–N3	285.1(5)
K–N1	296.3(6)	K–N3	282.5(5)
K–N2	304.5(5)		
C1–N1	109.5(8)		
C1–N2	131.4(8)	C1-N2-C2	118.0(7)
C2–N2	127.7(7)	N1-C1-N2	165(1)
C2–N3	116.9(6)	N2-C2-N3	172.0(9)
γ-K[N(CN)$_2$]			
K–N1	283(3) 2x	K–N1	285(3) 2x
K–N2	312(1) 2x	K–N2	289(1)
C1–N1	110(4)		
C1–N2	135(2)	C1-N2-C2	120(1)
C2–N2	142(2)	N1-C1-N2	169(3)
C2–N3	101(4)	N2-C2-N3	155(3)
β-Rb[N(CN)$_2$]			
Rb1–N1	296(1)	Rb2–N1	314(1)
Rb1–N1	305(1)	Rb2–N2	325(1)
Rb1–N2	301(1)	Rb2–N3	306(1)
Rb1–N3	311(1)	Rb2–N3	320(1)
Rb1–N4	300(1)	Rb2–N4	306(2)
Rb1–N5	308(2)	Rb2–N6	298(1)
Rb1–N6	298(1)	Rb2–N6	330(1)
C1–N1	117(2)	C3–N4	114(2)
C1–N2	135(2)	C3–N5	131(2)
C2–N2	130(2)	C4–N5	126(3)
C2–N3	118(2)	C4–N6	117(2)
C1-N2-C2	116(2)	C3-N5-C4	130(3)
N1-C1-N2	175(2)	N4-C3-N5	167(3)
N2-C2-N3	169(2)	N5-C4-N6	178(3)

The calculated density of α-K[N(CN)$_2$] is about 6% larger than that of β-K[N(CN)$_2$], while β-K[N(CN)$_2$] and γ-K[N(CN)$_2$] have nearly the same density. Accordingly the

0947-6539/01/0724-5378 $ 17.50+.50/0 *Chem. Eur. J.* **2001**, *7*, No. 24

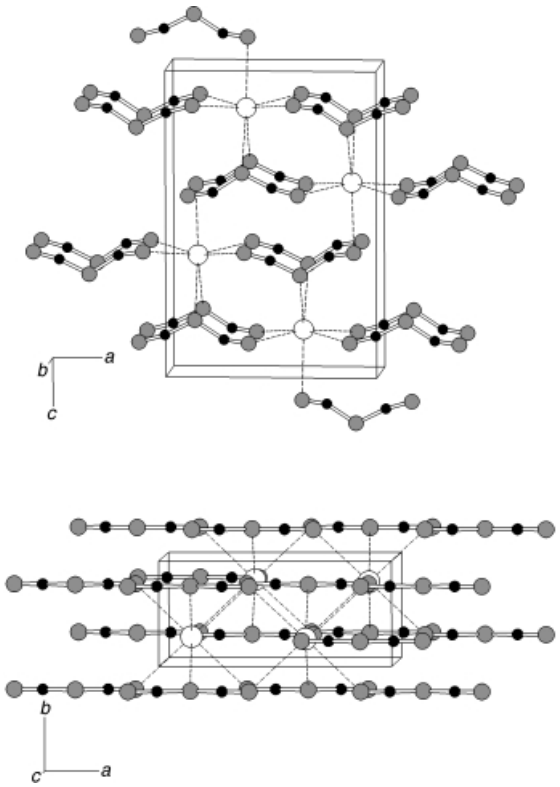

Figure 9. Top: Crystal structure of γ-K[N(CN)$_2$], view along [010] (K: open circles, C: black circles, N: gray circles). Bottom: Crystal structure of γ-K[N(CN)$_2$], view along [001] (K: open circles, C: black circles, N: gray circles).

K^+ ions are coordinated by eight N atoms in α-K[N(CN)$_2$], while in the high-temperature phases the K^+ ion is surrounded by seven N atoms. Similarly the average K^+–N distances in α-K[N(CN)$_2$] are larger than those in β-K[N(CN)$_2$] and γ-K[N(CN)$_2$]. In contrast to the polymorphs of Na[N(CN)$_2$] there is no tight structural similarity and no group–subgroup relationship between the space groups of the three modifications of K[N(CN)$_2$]; accordingly the phase transitions between them seem to be of first order.

$K_3[C_6N_9]$: The crystal structure of $K_3[C_6N_9]$ is built up of cyclic tricyanomelaminate ions $[C_6N_9]^{3-}$ that are connected by K^+ ions (Figure 10). The anions consist of a triazine ring with three N-C-N side-arms. One of these side-arms is turned reducing the idealized symmetry of the molecular anion from

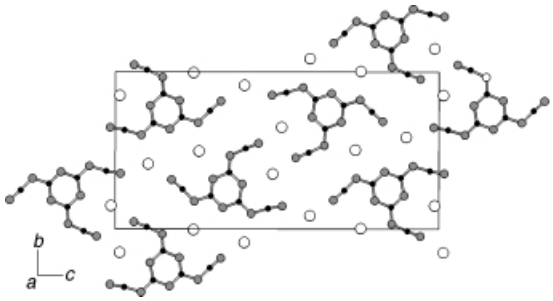

Figure 10. Crystal structure of $K_3[C_6N_9]$, view along [100] (K: open circles, C: black circles, N: gray circles). The crystal structure of $Rb_3[C_6N_9]$ is analogous.

C_{3h}, as found in $Na_3[C_6N_9]\cdot 3H_2O$,[24] to approximately C_s. There are three crystallographically different K^+ ions in the unit cell. K1 is surrounded by seven N atoms, while K2 and K3 are coordinated by eight N atoms, respectively. The average K^+–N distances amount to 295, 307, and 299 pm. As soft constraints were used for the refinement of the C and N atoms, the interatomic distances within the $[C_6N_9]^{3-}$ ions will not be discussed in detail.

In a projection along [100] (Figure 10) all tricyanomelaminate ions in $K_3[C_6N_9]$ seem to be oriented perpendicular to [100]. In this view the crystal structure of $K_3[C_6N_9]$ (space group $P2_1/c$) resembles that of $Na_3[C_6N_9]$ (space group $P2_1/n$) as viewed along [001]. However, in a projection along [010] (Figure 11) significant differences between both crystal structures became apparent: In the potassium compound both K^+ ions and $[C_6N_9]^{3-}$ ions are arranged in alternating layers parallel to the crystallographic plane (100). All $[C_6N_9]^{3-}$ ions are nearly parallel to each other and they are only slightly tilted out of (100). A similar arrangement of cations and $[C_6N_9]^{3-}$ ions in alternating layers is found in $M[HC_6N_9]\cdot 3H_2O$ ($M = Co^{2+}$, Ni^{2+}, Cu^{2+}, Cd^{2+})[25] and $Na_3[C_6N_9]\cdot 3H_2O$,[24] although in these compounds there are additional H_2O molecules in the layers. In $Na_3[C_6N_9]$ the anions are found in two orientations that are significantly tilted with respect to each other and out of the (001) plane; thus the anions do not really form layers.[3]

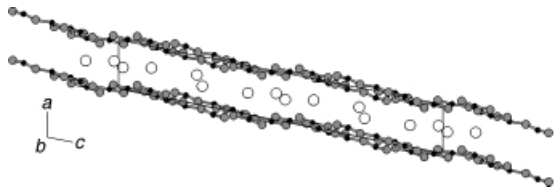

Figure 11. Crystal structure of $K_3[C_6N_9]$, view along [010] (K: open circles, C: black circles, N: gray circles).

The calculated density of $K_3[C_6N_9]$ (1.918 g cm^{-3}) is lower than that of $Na_3[C_6N_9]$ (1.972 g cm^{-3}), although potassium is the heavier homologue of sodium. Apparently the packing of cations and anions in $K_3[C_6N_9]$ leads to a less dense structure.

Thermal behavior of Rb[N(CN)$_2$]: The DSC curve of Rb[N(CN)$_2$] (Figure 2) is similar to that of K[N(CN)$_2$] showing an endothermic melting peak at 190 °C and a broad exothermic peak (onset: 260 °C) indicating the trimerization of the anions and the formation of $Rb_3[C_6N_9]$. With further heating, $Rb_3[C_6N_9]$ decomposes forming nondefined products. Even at −25 °C, α-Rb[N(CN)$_2$] slowly transforms to β-Rb[N(CN)$_2$].

α-Rb[N(CN)$_2$]: α-Rb[N(CN)$_2$] is isotypic with α-K[N(CN)$_2$]. Analogously the cations are coordinated by eight N atoms. The average Rb^+–N distance amounts to 313 pm (Table 8).

β-Rb[N(CN)$_2$]: Despite the fact that α-K[N(CN)$_2$] and α-Rb[N(CN)$_2$] are isotypic, β-Rb[N(CN)$_2$] does not crystallize in any structure type analogous to the other potassium dicyanamides. It has a rather complicated structure with 12

atoms in the asymmetric unit (Figure 12). There are two crystallographically independent Rb^+ ions and two $[N(CN)_2]^-$ anions. Both Rb^+ ions are coordinated by seven N atoms, the average Rb^+–N distances are 302 and 314 pm, respectively (Table 9). β-$Rb[N(CN)_2]$ does not form a layer structure. The planes of the N1-C1-N2-C2-N3 groups are orientated approximately parallel (010), while the N4-C3-N5-C4-N6 groups are nearly parallel (100).

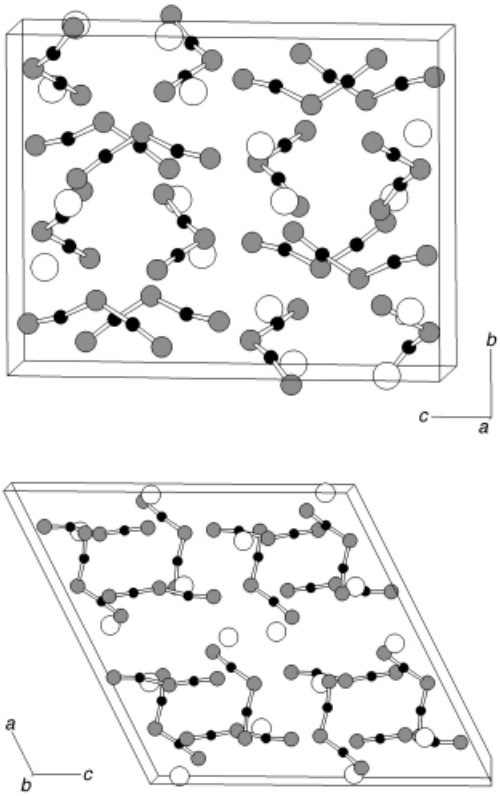

Figure 12. Top: Crystal structure of β-$Rb[N(CN)_2]$, view along [100] (Rb: open circles, C: black circles, N: gray circles). Bottom: Crystal structure of β-$Rb[N(CN)_2]$, view along [010] (Rb: open circles, C: black circles, N: gray circles).

Similar to the potassium dicyanamide the calculated density of the low-temperature phase is higher than that of the high-temperature phase, but the difference is not as large (2%). There is no group–subgroup relationship between the space groups of α- and β-$Rb[N(CN)_2]$.

$Rb_3[C_6N_9]$: $Rb_3[C_6N_9]$ is isotypic with $K_3[C_6N_9]$, the Rb^+ and $[C_6N_9]^{3-}$ ions form alternating layers. The number of N atoms coordinated to the Rb^+ ion is the same as in $K_3[C_6N_9]$; the average distances for Rb^+–N are 310 (Rb1), 317 (Rb2), and 312 pm (Rb3), respectively.

Discussion

The investigated alkali dicyanamides $M[N(CN)_2]$ (M = K, Rb) contain bent and planar anions. The point symmetry of these $[N(CN)_2]^-$ ions is approximately C_{2v}, although the crystallographic point symmetry is reduced to C_1 or C_s, respectively. The average distance between the C atoms and the bridging N atoms amounts to 133 pm, representing single bonds. The distances between C and the terminal N atoms are much shorter (average distance 113 pm) as they represent triple bonds. The N-C-N angles are nearly linear (average 170°) and the C-N-C angles are significantly bent (average 120°). The observed interatomic distances and angles correspond well with those found in $Cs[N(CN)_2]$[26] and $NaCs_2[N(CN)_2]_3$,[25] which previously have been investigated by single-crystal X-ray diffraction.

Both $K[N(CN)_2]$ and $Rb[N(CN)_2]$ are polymorphic. No group–subgroup relationship between the structures of the different modifications occurs, as the phase transitions are reconstructive. Thus they are assumed to be of first order. Phase transitions of compounds with large elongated anions are more common than those with small spherical anions.[20]

In the case of $Na[N(CN)_2]$, the trimerization of $[N(CN)_2]^-$ ions (onset at 320 °C) and the formation of $[C_6N_9]^{3-}$ ions occurs in the solid state.[3] In contrast, $K[N(CN)_2]$ and $Rb[N(CN)_2]$ melt at 232 and 190 °C, respectively, before the trimerization of their anions occurs (onset at 310 °C for $K[N(CN)_2]$ and at 260 °C for $Rb[N(CN)_2]$). To our knowledge, these are the first examples in which simple inorganic anions trimerize in the melt. A comparison of the crystal structures of β-$Na[N(CN)_2]$ and $Na_3[C_6N_9]$ gave no evidence for a preorientation of the dicyanamide ions in the solid before their trimerization. This is in accordance with the observation that $K_3[C_6N_9]$ and $Rb_3[C_6N_9]$ are formed by trimerization from the melt, in which a preorientation of three $[N(CN)_2]^-$ ions to form $[C_6N_9]^{3-}$ is unlikely. The differing thermal behavior of the three alkali dicyanamides seems to be due to their decreasing stability with increasing radius of the cations.

In contrast to the trimerization observed for the alkali dicyanamides, no evidence for an analogous transformation was found for the alkaline earth dicyanamides $M^{II}[N(CN)_2]_2$ (M^{II} = Mg, Ca, Sr, or Ba). Melting was not observed for these compounds nor for the transition metal dicyanamides, but the dicyanamides became X-ray amorphous irreversibly while heating at 300–500 °C.[4] Presumably, the higher charged alkaline earth cations prevent trimerization and increase the thermal stability compared with the alkali dicyanamides.

$K_3[C_6N_9]$ and $Rb_3[C_6N_9]$ are isotypic. Their cations and $[C_6N_9]^{3-}$ anions are arranged in approximately plane layers, which are only slightly sheared; this results in a monoclinic angle of about 100°. An idealized structure with all atoms of the layers situated on the mirror plane would be orthorhombic with the space group *Pmcn*. Reducing the symmetry by elimination of the mirror plane of this idealized structure leads to two possible monoclinic subgroups. If the glide plane *c* is maintained, the structure of $K_3[C_6N_9]$ and $Rb_3[C_6N_9]$ results, while maintaining the glide plane *n* leads to the structure of $Na_3[C_6N_9]$. Accordingly the structural similarities of $Na_3[C_6N_9]$, $K_3[C_6N_9]$, and $Rb_3[C_6N_9]$ can be explained by different symmetry reductions from a common aristotype.

Acknowledgements

The authors would like to thank W. Wünschheim (LMU München) for performing the DSC measurements. Financial support from the Fonds der Chemischen Industrie (Germany), the Bundesministerium für Bildung und

  0947-6539/01/0724-5380 $ 17.50+.50/0

Forschung (project 03-SC5LMU-5), and especially from the Deutsche Forschungsgemeinschaft (Gottfried-Wilhelm-Leibniz-Programm) is gratefully acknowledged.

[1] See for example: a) T. Malkow, *Mater. Sci. Eng. A*, **2001**, *302*, 311; b) E.-G. Wang, *Adv. Mater.* **1999**, *11*, 1129; c) S. Matsumoto, E.-Q. Xie, F. Izumi, *Diamond Relat. Mater.* **1999**, *8*, 1175; d) Y. Guo, W. A. Goddard, *Chem. Phys. Lett.* **1995**, *237*, 72; e) M. Coté, M. L. Cohen, *Phys. Rev. B* **1997**, *55*, 5684.
[2] U. Berger, W. Schnick, *J. Alloys Compd.* **1994**, *206*, 179.
[3] B. Jürgens, E. Irran, J. Schneider, W. Schnick, *Inorg. Chem.* **2000**, *39*, 665.
[4] B. Jürgens, E. Irran, W. Schnick, *J. Solid State Chem.* **2001**, *157*, 241.
[5] A. Purdy, E. Houser, C. F. George, *Polyhedron* **1997**, *16*, 3671.
[6] W. Madelung, E. Kern, *Liebigs Ann. Chem.* **1922**, *427*, 26.
[7] E. C. Franklin, *J. Am. Chem. Soc.* **1922**, *44*, 486.
[8] B. Bann, S. A. Miller, *Chem. Rev.* **1958**, *58*, 131.
[9] R. P. Subrayan, P. G. Rasmussen, *Trends Polym. Sci.* **1995**, *3*, 165.
[10] V. N. Khabashesku, J. L. Zimmerman, J. L. Margrave, *Chem. Mater.* **2000**, *12*, 3264.
[11] R. C. de Vries, *Mater. Res. Innovations* **1997**, *1*, 161.
[12] I. Alves, G. Demazeau, B. Tanguy, F. Weill, *Solid State Commun.* **1999**, *109*, 697.
[13] T. Komatsu, T. Nakamura, *J. Mater. Chem.* **2001**, *11*, 474.
[14] B. Jürgens, E. Irran, W. Schnick, unpublished results.
[15] J. W. Visser, *J. Appl. Crystallogr.* **1969**, *2*, 89.
[16] A. Altomare, M. C. Burla, G. Cascarano, C. Giacovazzo, A. Guagliardi, A. G. G. Moliterni, G. Polidori, *J. Appl. Crystallogr.* **1995**, *28*, 842.
[17] A. Altomare, G. Cascarano, C. Giacovazzo, A. Guagliardi, M. C. Burla, G. Polidori, M. Camalli, *J. Appl. Crystallogr.* **1994**, *27*, 435.
[18] A. C. Larson, R. B. von Dreele, General Structure Analysis System, Los Alamos National Laboratory Report LAUR 86–748, **1990**.
[19] Further details on the crystal structure investigations may be obtained from the Fachinformationszentrum Karlsruhe, 76344 Eggenstein-Leopoldshafen, Germany (fax: (+49)7247-808-666; e-mail: crysdata@fiz-karlsruhe.de) on quoting the depository numbers CSD-411930 (α-K[N(CN)$_2$]), CSD-411931 (β-K[N(CN)$_2$]), CSD-411932 (γ-K[N(CN)$_2$]), CSD-411933 ($K_3[C_6N_9]$), CSD-411934 (α-Rb[N(CN)$_2$]), CSD-411935 (β-Rb[N(CN)$_2$]), CSD-411936 ($Rb_3[C_6N_9]$).
[20] Y. Yamada, T. Watanabe, *Acta Crystallogr.* **1963**, *36*, 1032.
[21] J. A. A. Mokuolu, J. C. Speakman, *Acta Crystallogr. Sect. B* **1975**, *31*, 172.
[22] C. R. Kmety, Q. Huang, J. W. Lynn, R. W. Erwin, J. L. Manson, S. McCall, J. E. Crow, K. L. Stevenson, J. S. Miller, A. J. Epstein, *Phys. Rev. B* **2000**, *62*, 5576.
[23] C. R. Kmety, J. L. Manson, Q. Huang, J. W. Lynn, R. W. Erwin, J. S. Miller, A. J. Epstein, *Phys. Rev. B* **1999**, *60*, 60.
[24] B. Jürgens, W. Milius, P. Morys, W. Schnick, *Z. Anorg. Allg. Chem.* **1998**, *624*, 91.
[25] B. F. Abrahams, S. J. Egan, B. F. Hoskins, R. Robson, *Chem. Commun.* **1996**, 1099.
[26] P. Starynowicz, *Acta Crystallogr. Sect. C* **1991**, *47*, 2198.

Received: June 1, 2001 [F3310]